


ORIGINAL ARTICLE

UNC119 is a binding partner of tumor suppressor Ras-association domain family 6 and induces apoptosis and cell cycle arrest by MDM2 and p53

Hiroaki Iwasa¹ | Aradhan Sarkar¹ | Takano Shimizu¹ | Takeru Sawada¹ |
 Shakhawoat Hossain^{1,2} | Xiaoyin Xu^{1,3} | Junichi Maruyama¹ |
 Kyoko Arimoto-Matsuzaki¹ | Kanchanamala Withanage¹ | Kentaro Nakagawa¹ |
 Hidetake Kurihara⁴ | Hidehito Kuroyanagi⁵ | Yutaka Hata^{1,6} 

¹Department of Medical Biochemistry, Graduate School of Medical and Dental Sciences, Tokyo Medical and Dental University, Tokyo, Japan

²Department of Biochemistry and Molecular Biology, University of Rajshahi, Rajshahi, Bangladesh

³China Department of Breast Surgery, The Second Affiliated Hospital of Wenzhou Medical University, Wenzhou, Zhejiang, China

⁴Department of Physical Therapy, Faculty of Health Science, Aino University, Osaka, Japan

⁵Laboratory of Gene Expression, Medical Research Institute, Tokyo Medical and Dental University, Tokyo, Japan

⁶Center for Brain Integration Research, Tokyo Medical and Dental University, Tokyo, Japan

Correspondence: Yutaka Hata, Department of Medical Biochemistry, Graduate School of Medical and Dental Sciences, Tokyo Medical and Dental University, Tokyo, Japan (yuhammch@tmd.ac.jp).

Funding information

Japan Society for the Promotion of Science, Grant/Award Number: 26293061, 26460359

Ras-association domain family 6 (RASSF6) is a tumor suppressor that interacts with MDM2 and stabilizes p53. *Caenorhabditis elegans unc-119* encodes a protein that is required for normal development of the nervous system. Humans have 2 *unc-119* homologues, *UNC119* and *UNC119B*. We have identified *UNC119* as a RASSF6-interacting protein. *UNC119* promotes the interaction between RASSF6 and MDM2 and stabilizes p53. Thus, *UNC119* induces apoptosis by RASSF6 and p53. *UNC119* depletion impairs DNA repair after DNA damage and results in polyploid cell generation. These findings support that *UNC119* is a regulator of the RASSF6-MDM2-p53 axis and functions as a tumor suppressor.

KEYWORDS

apoptosis, MDM2, p53, RASSF, tumor suppressor

1 | INTRODUCTION

The human genome has 10 genes encoding proteins designated as Ras-association (RA) domain family (RASSF) proteins.¹⁻⁵ RASSF1 to RASSF6 have a RA domain near the C-terminal region and a coiled-coiled motif in the C-terminal region. This coiled-coil domain

is called the Salvador/RASSF/Hippo (SARAH) domain. RASSF7 to RASSF10 have a RA domain in the N-terminal region and lack the SARAH domain.^{6,7} RASSF1 to RASSF6 are collectively called C-RASSF, whereas RASSF7 to RASSF10 are named N-RASSF. C-RASSF proteins are regarded as tumor suppressors. *RASSF1A*, a major splicing variant of *RASSF1*, was identified in the lung tumor

This is an open access article under the terms of the Creative Commons Attribution-NonCommercial License, which permits use, distribution and reproduction in any medium, provided the original work is properly cited and is not used for commercial purposes.

© 2018 The Authors. *Cancer Science* published by John Wiley & Sons Australia, Ltd on behalf of Japanese Cancer Association.

suppressor locus.⁸ RASSF1A expression is frequently suppressed by hypermethylation in the promoter region in cancers, and its low expression is associated with poor prognosis.⁴ Other C-RASSF proteins including RASSF6 are also frequently downregulated in human cancers.⁴ The molecular mechanism underlying the tumor suppressive function of RASSF1A is well studied. RASSF1A stabilizes microtubules, regulates the G2/M checkpoint, and causes apoptosis and cell-cycle arrest through MDM2 and p53.^{9–13} RASSF1A interacts with mammalian Ste20-like kinases (MST1 and MST2) and activates the tumor suppressor Hippo pathway.^{14–16} These properties are partially, not entirely, shared by other C-RASSF proteins. RASSF6 interacts with MDM2, stabilizes p53, and induces apoptosis and cell-cycle arrest.¹⁷ RASSF6 forms a complex with MST1/2, but, in contrast to RASSF1A and MST2, RASSF6 and MST1/2 form a complex and inhibit each other under basal conditions.¹⁸ However, when certain stimuli, such as okadaic acid treatment, trigger dissociation of the complex, the Hippo pathway is activated and, simultaneously, RASSF6 induces apoptosis independently of the Hippo pathway. Thus, RASSF6 and the Hippo pathway cooperate with each other as tumor suppressors. Nevertheless, the mechanism by which RASSF6-mediated apoptosis is triggered is not yet clarified. Therefore, it is important to identify molecules that interact with and regulate RASSF6.

unc-119 was identified as 1 of the genes whose mutations cause uncoordinated movement in *Caenorhabditis elegans*.¹⁹ The human *UNC119* gene was found as a retina-enriched gene and named human retina gene 4 (HRG4).²⁰ The gene is registered as *UNC119* in the database of the National Center for Biotechnology Information (ID:9094). Truncation mutation of *UNC119* is detected in human patients and causes retinal degeneration in transgenic mice.²¹ Humans have another closely related gene, *UNC119B* (ID:84747).²² *UNC119* is frequently depicted as *UNC119A* in research papers. To avoid confusion, we will also use *UNC119A* for the gene and *UNC119A* for the protein in this report. *UNC119A* has two splicing variants, *UNC119Aa* and *UNC119Ab*, which encode different amino acids in the C-terminal sequences.²³ *UNC119A* is localized at a ribbon synapse in retina.²⁰ *UNC119A* is similar in structure to lipid-binding proteins, cGMP phosphodiesterase (PDE δ), and Rho GDP dissociation inhibitor (RhoGDI).²⁴ Lipid-modified proteins such as transducin, Lyn, Fyn, Abl1, and Abl2 interact with *UNC119A*.²⁵ Another important binding partner is RIBEYE, a major component of ribbon synapse.²⁶ *UNC119B* is implicated in the transport of myristoylated nephrocystin-3.²² Through the interaction with these proteins, *UNC119A* and *UNC119B* play important roles in ribbon synapse formation, T-cell activation, and cilia formation.

We identified *UNC119A* as a RASSF6-binding partner. Endogenous *UNC119A* and RASSF6 are coimmunoprecipitated from human colon cancer SW480 cells and show a similar distribution in rat kidney. *UNC119A* promotes interactions between RASSF6 and MDM2 and regulates apoptosis and the cell cycle by p53. These findings suggest that *UNC119A* is implicated in the regulation of the RASSF6-MDM2-p53 axis.

2 | MATERIALS AND METHODS

Cell cultures and transfection. HEK293FT, HCT116, U2OS, SW480, HeLa, H1299, and TIG3 cells were cultured in Dulbecco's Modified Eagle Medium (DMEM) containing 10% fetal bovine serum and 10 mM HEPES-NaOH at pH 7.4 under 5% CO₂ at 37°C. DNA transfection was performed with Lipofectamine 2000 (Thermo Fisher Scientific). HCT116 p53^{-/-} cells were infected with lentivirus vector (lenti-CRSIPR-MDM2-CR) and selected with puromycin. Clones were isolated and MDM2 depletion was confirmed by the immunoblotting. Other Materials and methods are described in Doc S1.

3 | RESULTS

3.1 | RASSF6 interacts with UNC119A

We obtained *UNC119A* as a putative RASSF6-binding partner through yeast 2-hybrid screening with human kidney cDNA library. To detect interaction between endogenous RASSF6 and *UNC119A*, we used human colon cancer SW480 cells, which express both RASSF6 and *UNC119A* at a high level (Figure 1A). RASSF6 was coimmunoprecipitated with *UNC119A* (Figure 1B). We previously characterized the localization of RASSF6 in rat kidney and showed that RASSF6 is detected in the renal glomerulus and renal tubular epithelial cells.²⁷ We immunostained rat kidney with anti-*UNC119A* antibody. *UNC119A* signals were detected in the renal glomerulus (Figure 1C). In the glomerulus, RASSF6 and *UNC119A* were partially colocalized with nephrin and synaptopodin, which are markers of the slit diaphragm. Like RASSF6, *UNC119A* was also detected in renal tubular epithelial cells. These findings support that *UNC119A* and RASSF6 are similarly distributed in the renal glomerulus and renal tubular epithelial cells.

3.2 | RASSF6 interacts with UNC119A, but not with UNC119B

UNC119A has two splicing variants, *UNC119Aa* and *UNC119Ab*.²³ Myc-*UNC119Aa* and Myc-*UNC119Ab* were equally coimmunoprecipitated with FLAG-RASSF6 from HEK293FT cells (Figure 2A). *UNC119B* did not bind to RASSF6 under the same condition that *UNC119Ab* interacted with RASSF6 (Figure 2B). We confirmed the results in the reverse immunoprecipitations. FLAG-RASSF6 was coimmunoprecipitated with Myc-*UNC119Aa* and Myc-*UNC119Ab*, but not with Myc-*UNC119B* (Figure 2C,D). We used *UNC119Ab* (hereafter named *UNC119A*) for the following studies. We further confirmed that GST-*UNC119A* as well as GST-MDM2 bound MBP-RASSF6 in vitro, supporting the direct interaction between *UNC119A* and RASSF6 (Figure 2E). We next compared the subcellular distribution of *UNC119A* and RASSF6. In the subcellular fractionation, exogenously expressed *UNC119A* and RASSF6 were recovered in both the cytoplasmic and nuclear fractions (Figure 2F, left). Interaction between *UNC119A* and RASSF6 was observed in

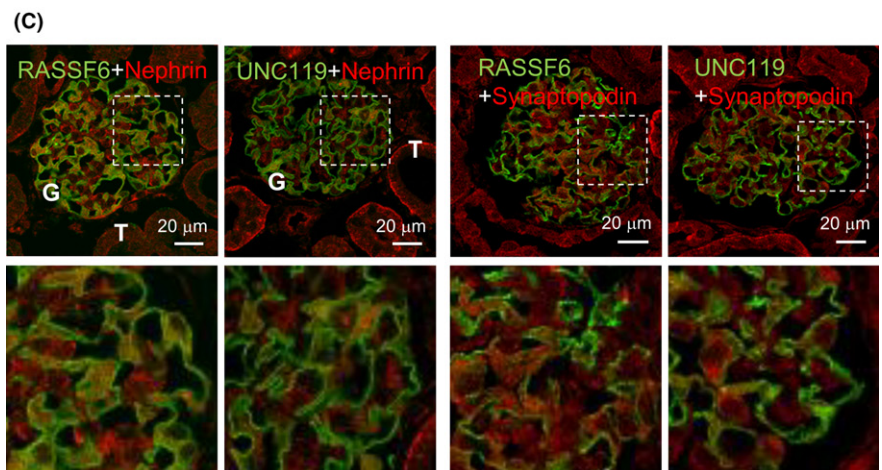
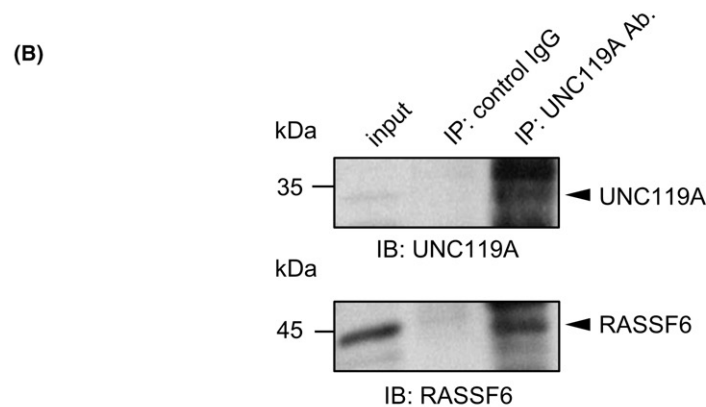
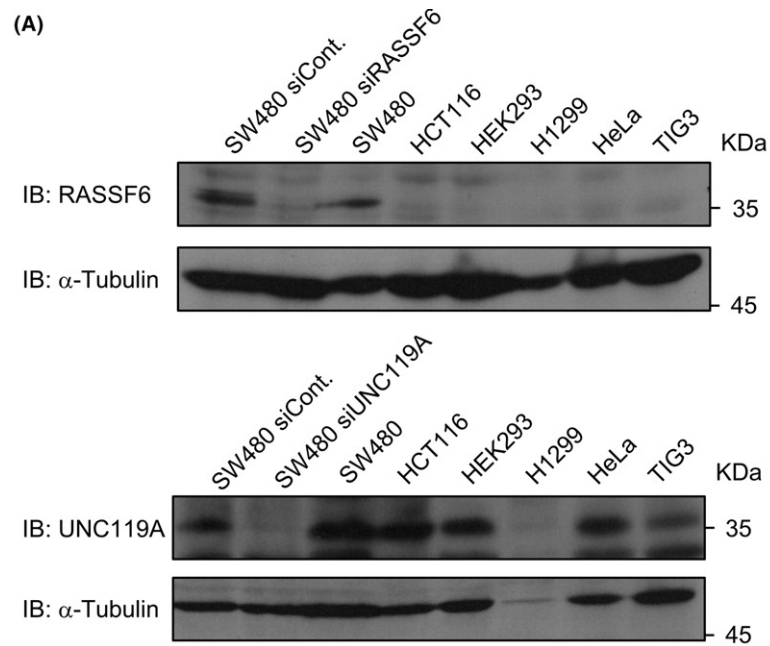


FIGURE 1 Interaction between Ras-association domain family 6 (RASSF6) and UNC119A and the localization of UNC119A in rat kidney. A, RASSF6 and UNC119A in various cell lines. Whole-cell lysates of indicated cell lines (50 μ g total protein) were immunoblotted by anti-RASSF6 and anti-UNC119A antibodies. RASSF6 was detected in SW480 cells only. RASSF6 knockdown abolished the signal detected by anti-RASSF6 antibody in SW480 cells (second lane). UNC119A was detected in SW480, HCT116, HEK293FT, H1299, HeLa, and TIG3 cells. UNC119A knockdown abolished signals detected by anti-UNC119A antibody (second lane). B, UNC119A was immunoprecipitated from SW480 cells and immunoblotted with anti-UNC119A and anti-RASSF6 antibodies. C, Rat kidney was immunostained with the indicated antibodies. UNC119A (green) and RASSF6 (green) were detected in the glomerulus (G) and in the renal tubules (T). Demarcated areas are shown at higher magnification in the lower row. UNC119A and RASSF6 are partially overlapped by nephrin (red) and synaptopodin (red). Bar, 20 μ m

both fractions (Figure 2F, left). In contrast, MDM2, even when exogenously expressed, was mainly recovered in the nuclear fraction (Figure 2F, right). As a matter of course, the interaction between RASSF6 and MDM2 took place in the nuclear fraction. Proximity ligation assay also supported the interaction between UNC119A and RASSF6 in the cytoplasm and the nucleus (Figure 2G).

3.3 | UNC119A induces apoptosis depending on p53 and RASSF6 and is implicated in UV-induced apoptosis

RASSF6 induces apoptosis and cell-cycle arrest.¹⁷ This function of RASSF6 partly depends on p53. We raised the question of whether

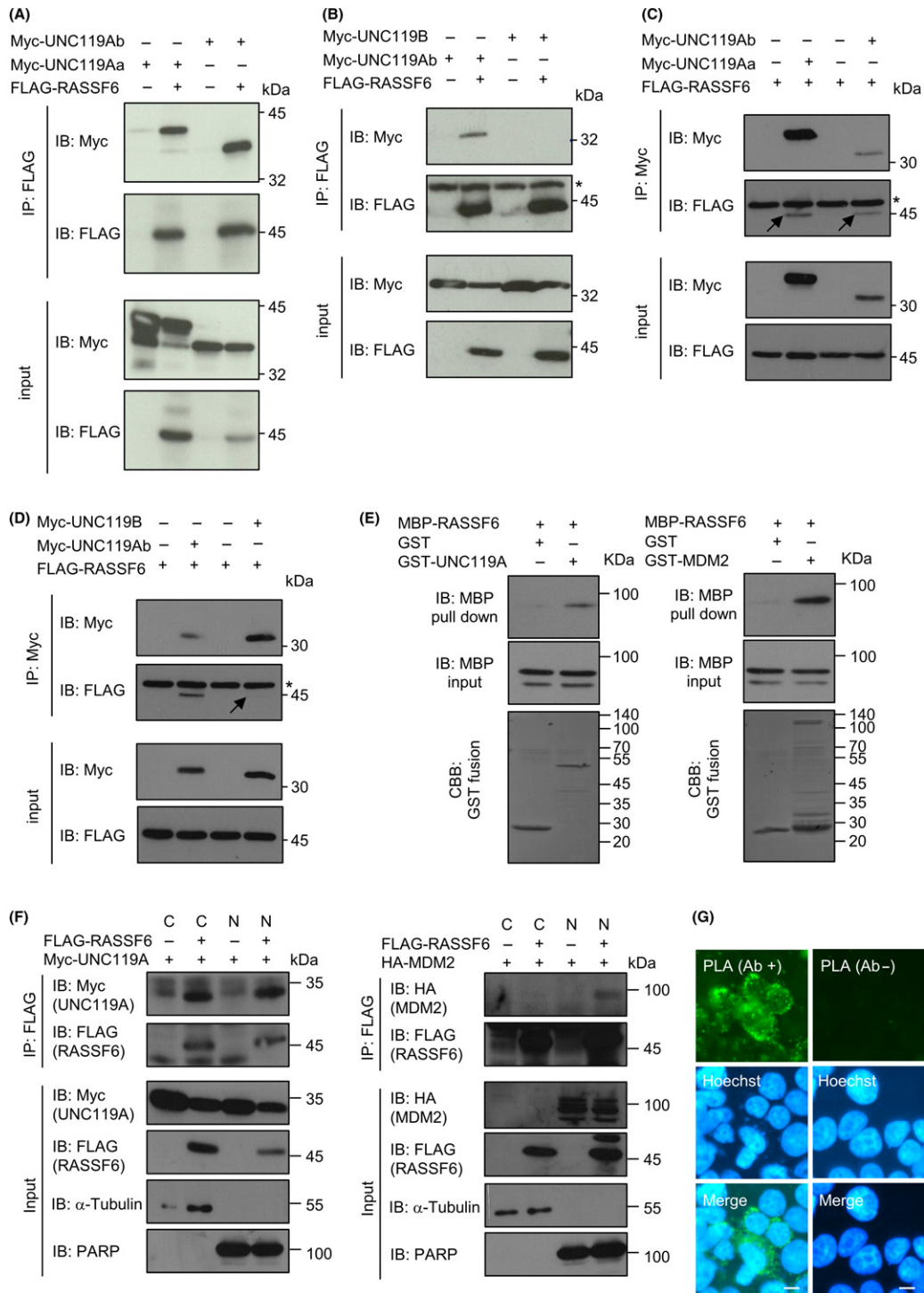


FIGURE 2 Interaction between Ras-association domain family 6 (RASSF6) and UNC119A variants. HEK293FT cells were transfected with pCleoMyc-UNC119Aa, pCleoMyc-UNC119Ab, pCleoMyc-UNC119B, and pCleoMyc-FHF-RASSF6. Immunoprecipitation was conducted with anti-DYKDDDDK (1E6) beads in (A), and (B), and with anti-Myc antibody in (C) and (D). A, B, Myc-UNC119Aa and Myc-UNC119Ab were coimmunoprecipitated with FLAG-RASSF6, but Myc-UNC119B was not. Asterisks indicate the immunoglobulin. C, D, FLAG-RASSF6 was coimmunoprecipitated with Myc-UNC119Aa and Myc-UNC119Ab (arrows in (C)), but not with Myc-UNC119B (arrow in (D)). E, Eluted MBP-RASSF6 was incubated with control GST, GST-UNC119A, and GST-MDM2 fixed on glutathione cellulose beads. MBP-RASSF6 attached to beads was detected with anti-MBP antibody. Lower panels show GST proteins in Coomassie Brilliant Blue staining. F, FLAG-RASSF6, Myc-UNC119A, and HA-MDM2 were expressed in HEK293FT cells. Subcellular fractionation was carried out. Immunoprecipitation was conducted by use of anti-DYKDDDDK (1E6) beads from the cytoplasmic and nuclear fractions. α -Tubulin and anti-poly (ADP-ribose) polymerase (PARP) were used as cytoplasmic and nuclear markers, respectively. UNC119A was coimmunoprecipitated with RASSF6 in both the cytoplasmic and nuclear fractions, whereas MDM2 was coimmunoprecipitated in the nuclear fraction. G, Myc-UNC119A and FLAG-RASSF6 were expressed in HEK293FT cells. Proximity ligation assay was carried out according to the manufacturer's protocol. The image without the antibody is also shown as a control. Bars, 10 μ m

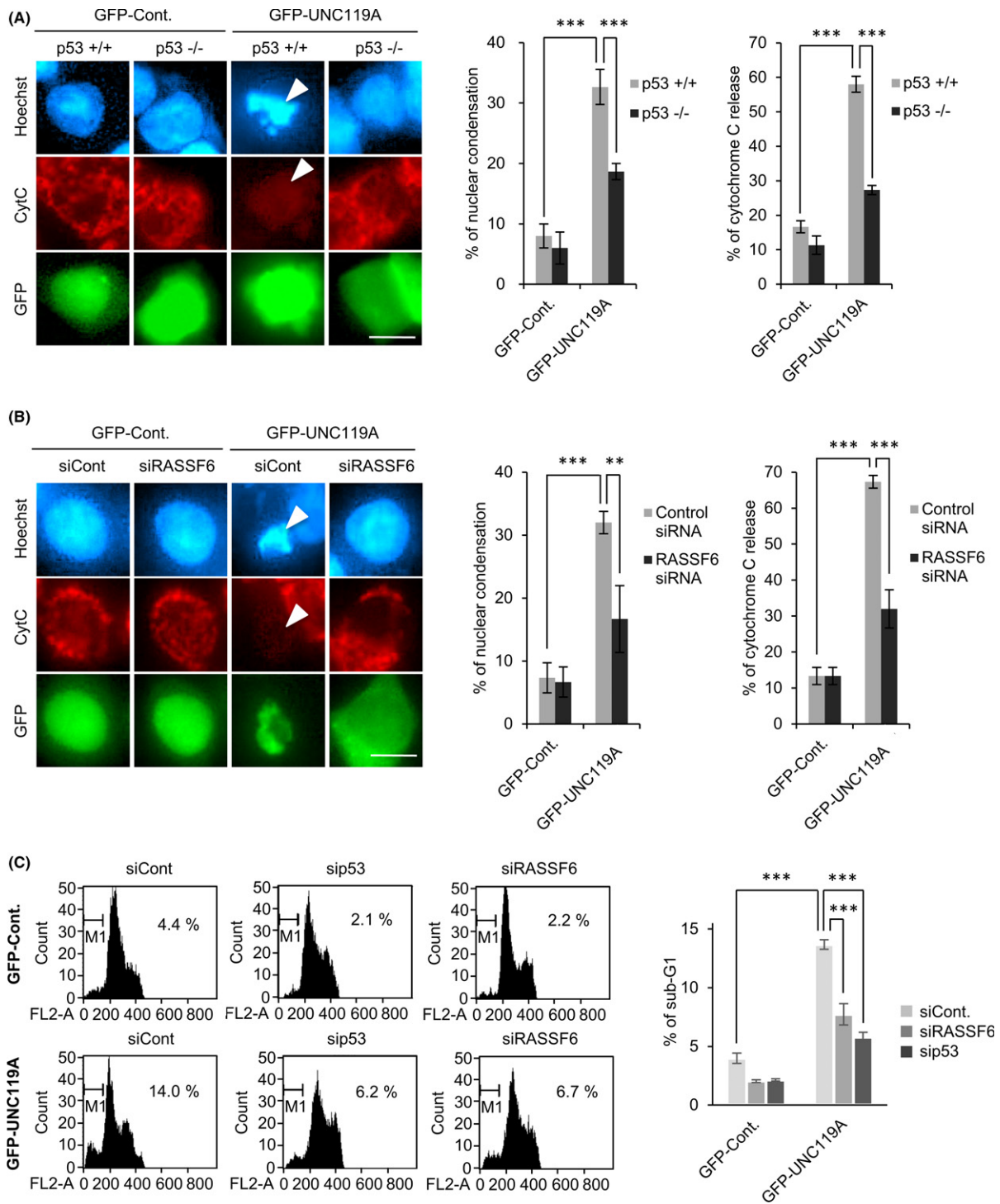


FIGURE 3 UNC119A-induced apoptosis depends on Ras-association domain family 6 (RASSF6) and p53. A, p53-positive- (p53 +/+) and p53-negative- (p53 -/-) HCT116 cells were transfected with pBudGFP-SUMO (GFP-Cont.) or pCneoGFP-UNC119A. 24 h later, cells were immunostained with anti-cytochrome-C antibody. Nuclei were visualized with Hoechst 33342. Cytochrome-C remained in mitochondria in HCT116 cells expressing control GFP and HCT116 p53-/- cells expressing GFP-UNC119A. In HCT116 p53 +/+ cells, GFP-UNC119A-induced nuclear condensation and cytochrome-C release (arrowheads). 50 GFP-positive cells were observed in 3 independent experiments and cells with nuclear condensation and with cytochrome-C release were counted. Data are shown as mean with SEM. ****P* < .001. Bar, 10 μm. B,C, HCT116 cells were transfected with control or RASSF6-targeted siRNA. 72 h later, cells were transfected with pBudGFP-SUMO (GFP-Cont.) or pCneoGFP-UNC119A. In (B), 24 h later, apoptosis was evaluated as described for Figure 3A. GFP-UNC119A induced nuclear condensation and cytochrome-C release in control cells (arrowheads) but not in RASSF6-depleted cells. Data are shown as mean with SEM. ***P* < .01; and ****P* < .001. Bar, 10 μm. In (C), 24 h later, the cells were harvested. The sub-G1 population was evaluated with FACS. Numbers indicate the percentages of the sub-G1 population. GFP-UNC119A increased the sub-G1 population, but knockdown of p53 or RASSF6 reduced it. ****P* < .001

UNC119A induces apoptosis and, if it does, whether UNC119A-induced apoptosis is mediated by RASSF6 and p53. UNC119A overexpression caused nuclear condensation and cytochrome-C release in p53-positive HCT116 cells (Figure 3A, arrowheads). Ratios of cells with nuclear condensation and cytochrome-C release were smaller in p53-negative HCT116 cells (Figure 3A right graphs). RASSF6 depletion attenuated UNC119A-induced nuclear condensation and cytochrome-C release (Figure 3B). FACS analysis indicated an increase in the sub-G1 population in UNC119A-expressing HCT116 cells, but the depletion of p53 or RASSF6 suppressed it (Figure 3C). UV exposure increased the sub-G1 population from 3.88% to 59.38% (Figure 4, siCont, No treatment, and UV treatment). As previously reported, depletion of p53 or RASSF6 suppressed UV-induced sub-G1

population (Figure 4, siRASSF6 and sip53).¹⁷ Likewise, UNC119A depletion suppressed UV-induced the sub-G1 population (Figure 4A, siUNC119A#1). Another siRNA against *UNC119A* (siUNC119A#2) showed a similar effect (Figure S1A). The knockdown efficiencies were similar for both siRNAs (Figure 4B). These findings support that UNC119A regulates apoptosis by RASSF6 and p53.

3.4 | UNC119A induces cell-cycle arrest depending on RASSF6 and p53

We next tested the function of UNC119A in cell-cycle regulation. We expressed UNC119A in p53-positive HCT116 cells, which blocked BrdU incorporation (Figure 5A, siCont, arrowheads).

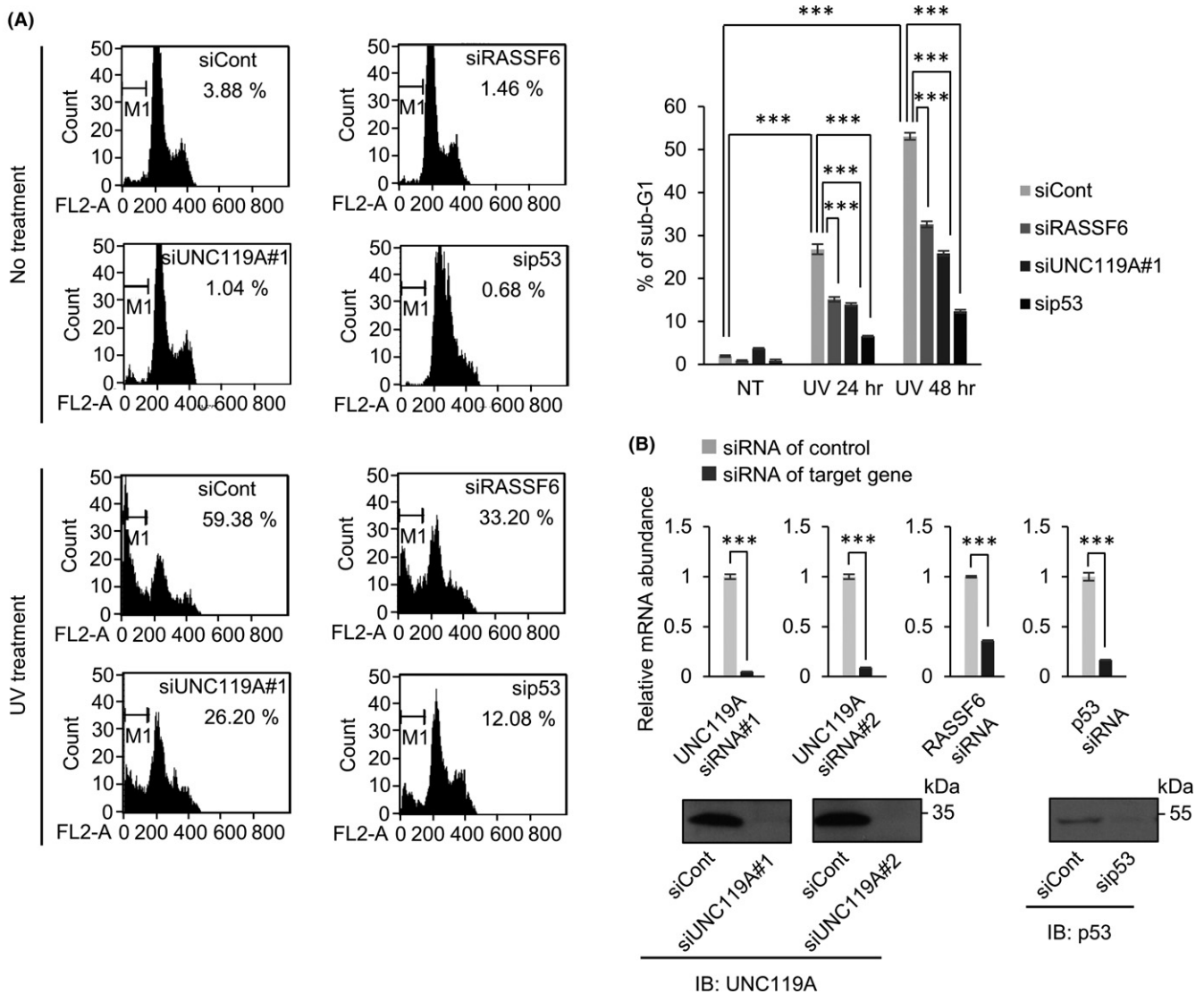


FIGURE 4 UNC119A is implicated in UV-induced apoptosis. A, HCT116 cells were transfected with control, UNC119A- (#1), Ras-association domain family 6 (RASSF6-), or *TP53*-targeted siRNA. 72 h later, cells were exposed to 25 J/m² ultraviolet (UV). 24 h and 48 h later, cells were harvested and the sub-G1 population was evaluated as described for Figure 3C. Left panel shows the results at 24 h. Numbers indicate the percentages of the sub-G1 population. ****P* < .001. B, Validation of the knockdown by *UNC119A*-, *RASSF6*-, and *TP53*-targeted siRNAs. HCT116 cells were harvested 72 h after transfection. qRT-PCR was carried out by use of GAPDH as a reference. ****P* < 0.001. Cell lysates (50 μg/total protein) were immunoblotted with anti-UNC119A and anti-p53 antibodies

Knockdown of p53 or RASSF6 recovered BrdU incorporation in UNC119A-expressing cells (Figure 5A, sip53 and siRASSF6, arrowheads). UNC119A reduced BrdU incorporation even in HCT116 p53^{-/-} cells, although the inhibitory effect was less remarkable (Figure S2). UV exposure induced G1/S arrest (Figure 5B, white arrow). UNC119A-depleted cells overrode the arrest, and the cell cycle proceeded 20 hours later (Figure 5B, black arrow). Another siRNA against UNC119A (siUNC119A#2) showed a similar effect (Figure S1B).

3.5 | UNC119A depletion suppresses p53-dependent transcription after UV exposure

We surmised that UNC119A plays a role in UV-induced p53-dependent apoptosis and cell-cycle arrest. To confirm this assumption, we quantified p53 target genes. UV exposure upregulated PUMA, CDKN1A, and BTG2 (Figure 5C). UNC119A depletion abrogated the UV-induced enhancement of these genes. We treated HCT116 cells with 10 μ mol/L VP-16 for 24 hours and observed an increase in p21, PUMA, BAX, and BTG3 in western blotting (Figure 5D, first and third lanes). UNC119A itself was slightly enhanced by VP-16. UNC119A silencing abolished the enhancement of these proteins (Figure 5D, third and fourth lanes).

3.6 | UNC119A regulates the stability of p53 by MDM2

We previously reported that RASSF6 blocks MDM2-mediated p53 degradation.¹⁷ We hypothesized that UNC119A regulates apoptosis and cell-cycle progression through RASSF6-MDM2-p53. To test this hypothesis, we examined the effect of UNC119A on the RASSF6-MDM2-p53 axis. UNC119A coexpression increased p53 expression (Figure 6A, left). To evaluate endogenous p53, we used TIG3 cells, in which p53 induces senescence. Endogenous p53, BAX, and p21 were, indeed, enhanced by UNC119A in TIG3 cells (Figure 6A, right). p53 degradation by treatment with cycloheximide was facilitated by UNC119A silencing (Figure 6B). Another siRNA against UNC119A (siUNC119A#2) showed a similar effect (Figure S1C). UNC119A depletion by siUNC119A#1 or #2 attenuated UV-induced enhancement of p53 (Figure 6C). p53 expression was remarkably enhanced by MDM2 depletion, and the additional knockdown of UNC119A did not affect p53 expression (Figure 6D). We prepared MDM2-depleted cells (MDM KO cells) from HCT116 p53^{-/-} cells by the CRISPR/Cas9 system and reintroduced p53 to evaluate the effect of UNC119A depletion on p53 expression. UNC119A depletion attenuated p53 expression in parent HCT116 p53^{-/-} cells (Figure 6E, first and second lanes). p53 expression was enhanced in MDM2 KO cells (Figure 6E, third lane). UNC119A silencing did not significantly affect p53 expression in MDM2 KO cells (Figure 6E, fourth lane). Likewise, UNC119A depletion did not decrease p53 expression by treatment with Nutlin-3, an inhibitor of MDM2 (Figure 6F). These findings support that MDM2 is implicated in the rapid degradation of p53 in the UNC119A-negative background.

3.7 | UNC119A strengthens the interaction between RASSF6 and MDM2

UNC119A enhances the stability of p53 and regulates apoptosis and cell-cycle progression by RASSF6 and p53. RASSF6 binds MDM2 and blocks MDM2-mediated p53 degradation.¹⁷ These findings prompted us to examine the effect of UNC119A on the interaction between RASSF6 and MDM2. HA-MDM2 was more efficiently coimmunoprecipitated with FLAG-RASSF6 in the presence of Myc-UNC119A (Figure 7A, left, white arrowhead). In the reverse immunoprecipitation, GFP-RASSF6 was more efficiently coimmunoprecipitated with FLAG-MDM2 in the presence of Myc-UNC119A (Figure 7A, middle, white arrowhead). In contrast to Myc-UNC119A, Myc-UNC119B did not enhance the interaction between HA-MDM2 and FLAG-RASSF6 (Figure 7A, right, white arrowhead).

3.8 | Effect of UNC119A on the interaction between MDM2 and p53 and on MDM2-dependent ubiquitination

We next examined the effect of UNC119A on the interaction between MDM2 and p53. For this purpose, we carried out the LUMIER assay by using luciferase-fused p53 (Luc-p53). Luc-p53 was coimmunoprecipitated with FLAG-MDM2 in the presence or absence of Myc-UNC119A. Luciferase activity detected in the immunoprecipitate was not changed by Myc-UNC119A (Figure 7B). Nevertheless, UNC119A decreased MDM2-mediated ubiquitination of p53 (Figure 7C). This finding is consistent with the previous observation that RASSF6 does not block the interaction between MDM2 and p53, but attenuates MDM2-mediated ubiquitination of p53.²⁸

3.9 | UNC119A depletion leads to the generation of polyploid cells

RASSF6 is important for DNA repair and prevents genomic instability.¹⁷ In the final set of experiments, we tested whether and how UNC119A is involved in DNA repair after DNA damage. HCT116 cells induced the expression of γ -H2A.X, a hallmark of DNA damage, after exposure to VP-16, a topoisomerase inhibitor. In control cells, γ -H2A.X decreased in a time-dependent way (Figure 8A). In UNC119A-depleted cells, γ -H2A.X was detected even under the basal condition (Figure 8A, left, siUNC119A#1, NT; right, immunoblot). Consistently, UNC119 silencing induced the phosphorylation of ATM without VP-16 treatment (Figure 8A, right, lower immunoblot, arrow). γ -H2A.X remained detectable even at 24 hours after VP-16 removal in UNC119A-depleted cells (Figure 8A, left). Another siRNA against UNC119A (siUNC119A#2) showed a similar effect on DNA repair (Figure S1D). We further cultured HCT116 cells that were exposed to VP-16 and analyzed DNA content with FACS. UNC119A depletion generated polyploid cells after exposure to VP-16 (Figure 8B). We also treated the cells with doxorubicin. UNC119A depletion increased polyploid cells in doxorubicin-treated cells (Figure 8C). Finally, we examined whether UNC119A suppression causes poor prognosis in human cancers by using the Prognoscan database

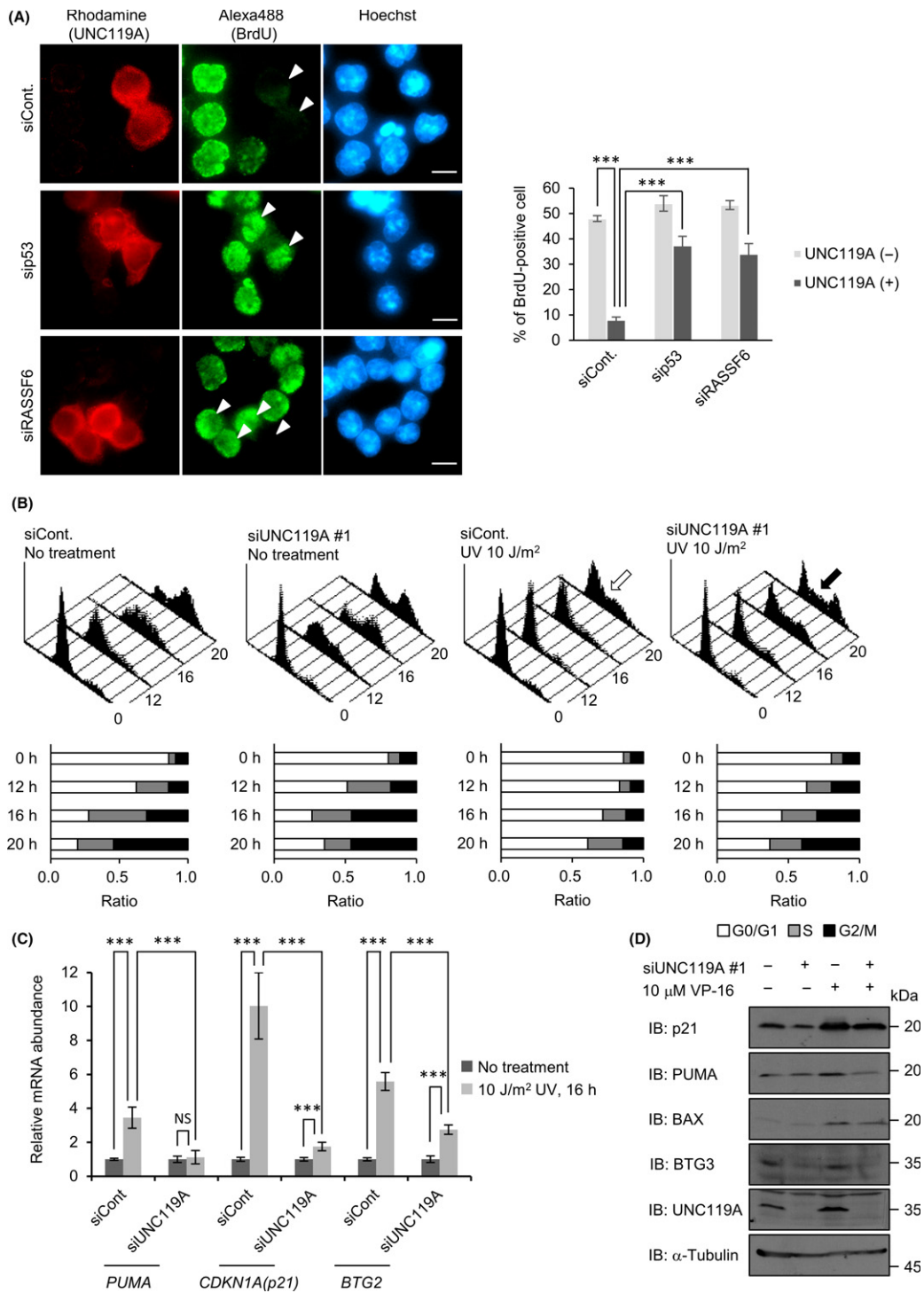


FIGURE 5 UNC119A-induced cell-cycle arrest depends on Ras-association domain family 6 (RASSF6) and p53 and UNC119A is implicated in UV-induced cell-cycle arrest. A, p53 or RASSF6 was knocked down in HCT116 cells. 72 h later, cells were transfected with pCIneoMyc-UNC119A. 24 h later, cells were incubated in the medium containing 10 μmol/L BrdU for 1 h. BrdU was detected by use of BrdU labeling and detection kit (Sigma-Aldrich, St Louis, MO, USA). Cells were immunostained with anti-BrdU (green) and anti-Myc (red) antibodies. Nuclei were visualized with Hoechst 33342. Cells expressing Myc-UNC119A (arrowheads) did not incorporate BrdU, whereas cells without Myc-UNC119A did (siCont). When p53 or RASSF6 was knocked down, Myc-positive cells also incorporated BrdU (sip53 and siRASSF6, arrowheads). B-D, HCT116 cells were transfected with control or UNC119A-targeted (#1) siRNA. In B, 72 h later, cells were transferred to the medium without serum for synchronization. 24 h later, cells were exposed to 10 J/m² UV and were cultured in the medium with serum. Cells were harvested at 0 h, 12 h, 16 h, and 20 h and analyzed by FACS. UV-induced G1/S arrest (white arrow) in control cells, whereas UNC119A-depleted cells overrode G1/S arrest (black arrow). In (C), 72 h later, cells were exposed to 10 J/m² UV. 16 h later, cells were harvested. qRT-PCR was carried out by use of GAPDH as a reference. UV exposure enhanced *PUMA*, *CDKN1A* (*P21*), and *BTG2* mRNAs and UNC119A knockdown blocked the enhancement. ****P* < .001. In D, HCT116 cells were treated with 10 μmol/L VP-16. 24 h later, cell lysates were immunoblotted with indicated antibodies

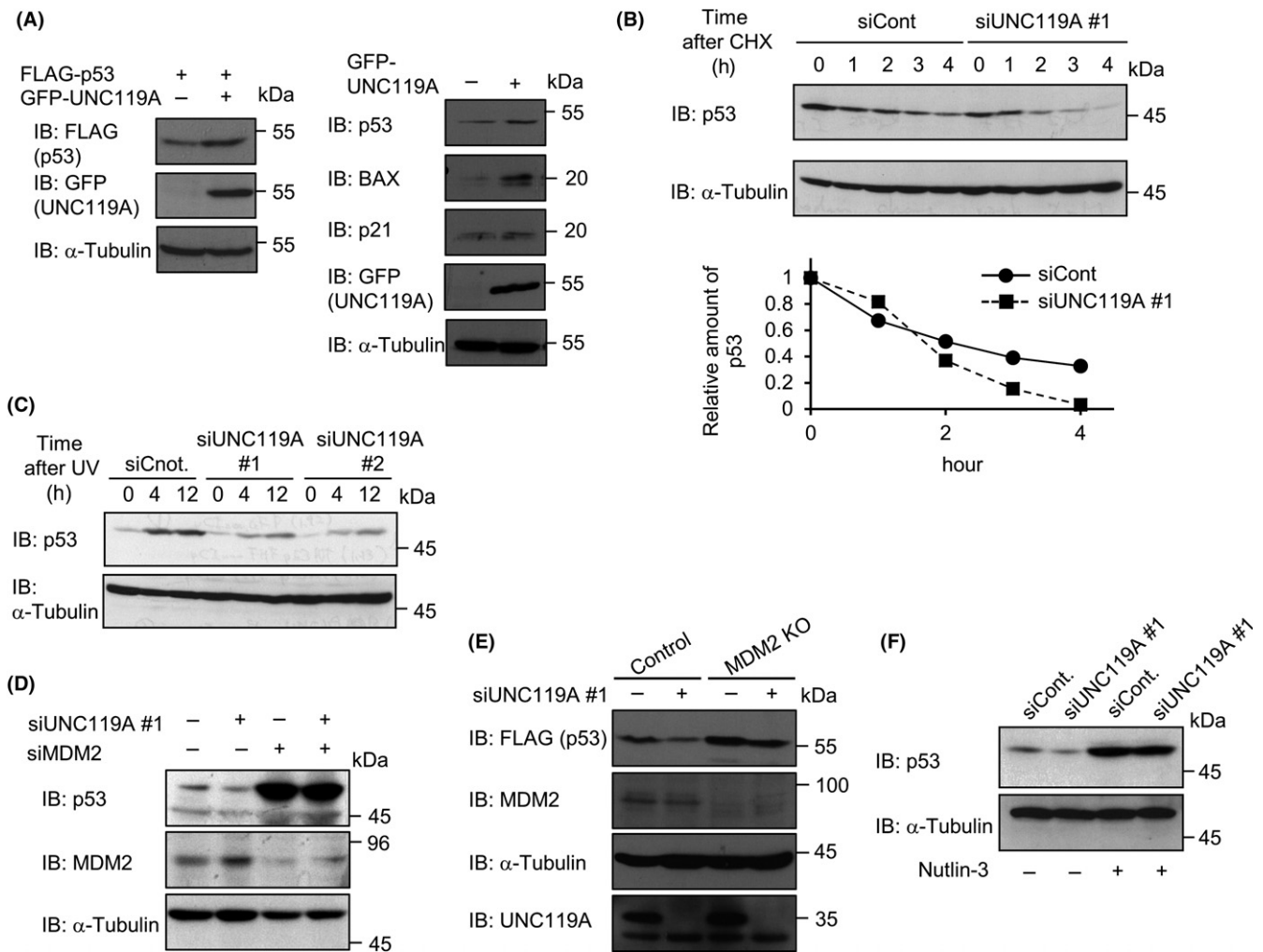


FIGURE 6 UNC119A stabilizes p53. A, FLAG-p53 was expressed in HEK293FT cells with or without GFP-UNC119A. p53 expression was enhanced by GFP-UNC119A (left). GFP-UNC119A was expressed in TIG3 cells (right). Endogenous p53, BAX, and p21 were detected. B, HCT116 cells were transfected with control or *UNC119A*-targeted siRNA #1. 72 h later, cells were treated with 50 mg/L cycloheximide. Endogenous p53 was detected at the indicated periods of time. Signals were measured by ImageJ. The signal at time 0 was set at 1.0. C, HCT116 cells were transfected with control or *UNC119A*-targeted (#1 and #2) siRNAs. 72 h later, cells were exposed to 10 J/m² UV. Endogenous p53 was detected at the indicated periods of time. D, HCT116 cells were transfected with control, *UNC119A*-targeted (#1), and/or *MDM2*-targeted siRNAs. 72 h later, cells were treated with 50 mg/L cycloheximide and, 4 h later, cells were harvested. Cell lysates were immunoblotted with indicated antibodies. E, *MDM2*-depleted HCT116 p53^{-/-} cells (*MDM2* KO cells) were prepared by CRISPR/CAS9 technology. *UNC119A* was further knocked down in parent HCT116 p53^{-/-} cells and *MDM2* KO cells (siUNC119A #1). FLAG-p53 was exogenously expressed in these cells. *UNC119A* silencing did not reduce p53 expression in *MDM2* KO cells. (F) HCT116 cells were transfected with control or *UNC119A*-targeted (#1) siRNA. 72 h later, the cells were treated with DMSO or 10 μmol/L Nutlin-3. 18 h later, the cells were harvested. Cell lysates were immunoblotted with the indicated antibodies

(<http://www.prognoscan.org>).²⁹ A total of 91 datasets provided information regarding *UNC119A*. In 6 datasets, low expression of *UNC119A* was associated with shorter overall or disease-free survival (Cox *P*-value < .05) (Figure 9).

4 | DISCUSSION

We carried out yeast 2-hybrid screening by use of *RASSF6* as bait and obtained *UNC119A*. *UNC119A* was coimmunoprecipitated with *RASSF6* from human colon cancer SW480 cells (Figure 1). The in

vitro binding assay supported the direct interaction between *RASSF6* and *UNC119A* (Figure 2). Although we could not demonstrate colocalization of endogenous *RASSF6* and *UNC119A* by double immunostaining, *RASSF6* and *UNC119A* showed similar distributions in rat kidney (Figure 1) and the proximity ligation assay also supported colocalization of *RASSF6* and *UNC119A* in cells (Figure 2). *UNC119A* binds *RASSF6*, whereas *UNC119B* does not (Figure 2). A previous study showed that *UNC119B*, but not *UNC119A*, regulates the transport of the myristoylated ciliopathy protein nephrocystin-3.²² Furthermore, *UNC119A* is reported to be localized to the centrosome, whereas *UNC119B* is not. This means

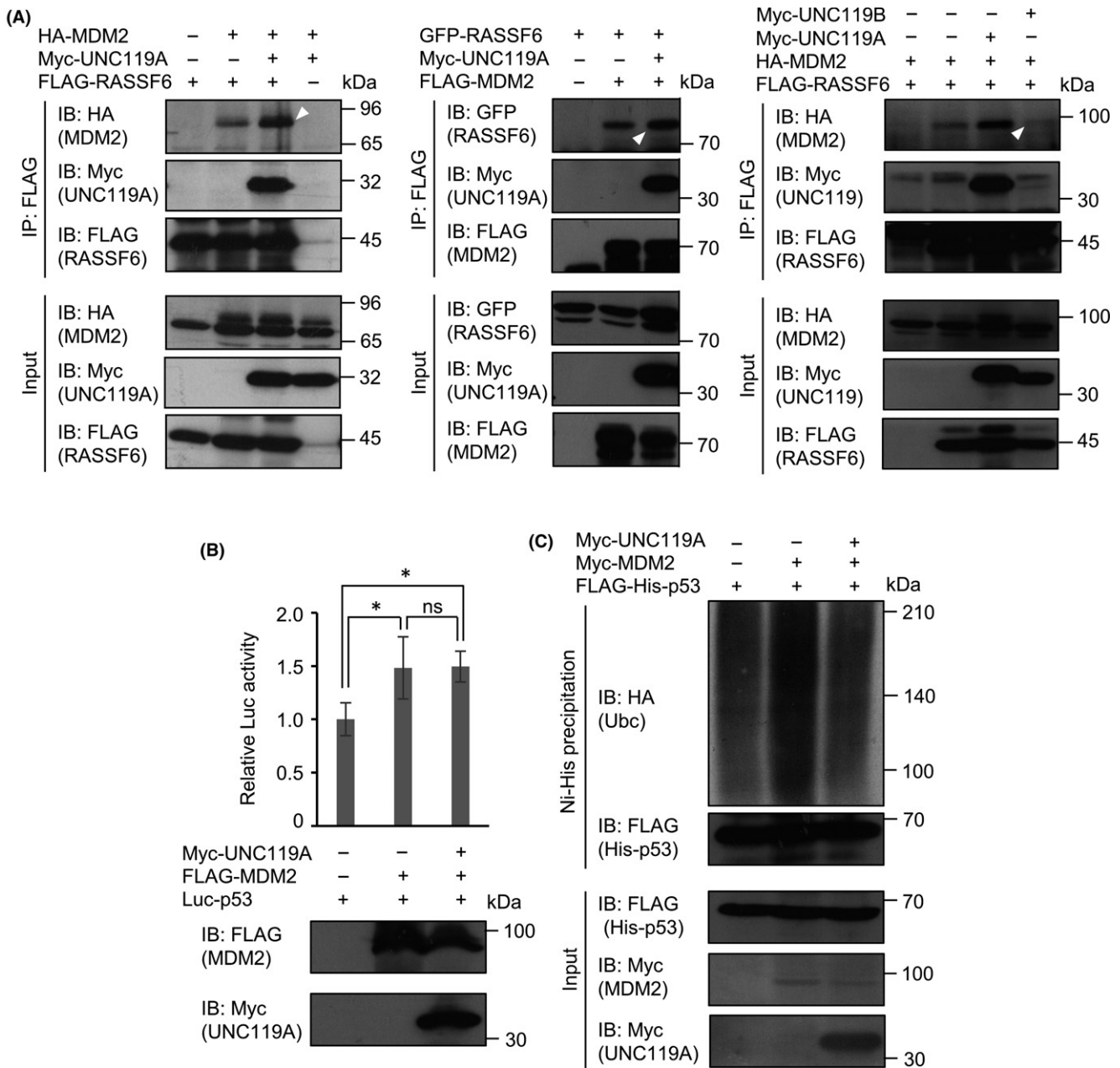


FIGURE 7 UNC119A enhances the interaction between Ras-association domain family 6 (RASSF6) and MDM2 and reduces p53 ubiquitination. A, HEK293FT cells were transfected with pCneoFHF-RASSF6 (FLAG-RASSF6), pCneoMyc-UNC119Ab (Myc-UNC119A), and pCneoHABA-MDM2 (HA-MDM2) as indicated (left). Immunoprecipitation was carried out with anti-DYKDDDDK (1E6) beads. Immunoprecipitates were immunoblotted with the indicated antibodies. UNC119A coexpression increased the coimmunoprecipitated HA-MDM2 (left, white arrowhead). Likewise, GFP-RASSF6, Myc-UNC119A, and FLAG-MDM2 were expressed in HEK293FT cells (middle). UNC119A coexpression increased the coimmunoprecipitated GFP-RASSF6 (middle, white arrowhead). In contrast to Myc-UNC119A, Myc-UNC119B did not increase the coimmunoprecipitated HA-MDM2 (right, white arrowhead). B, Luciferase-fused p53 (Luc-p53) was coimmunoprecipitated with FLAG-MDM2 in the presence or absence of Myc-UNC119A. Luciferase activity in the immunoprecipitates was measured. Lower panels show FLAG-MDM2 in the immunoprecipitates and Myc-UNC119A in the input. Data are shown as mean with SEM. * $P < .01$; ns, not significant. C, FLAG-His6-p53 and HA-UNC119A were expressed with Myc-UNC119A and Myc-MDM2 as indicated. Cells were harvested and FLAG-His6-p53 was precipitated by Ni-NTA beads. Immunoblottings were carried out with anti-HA antibody

that UNC119A and UNC119B are distinct in protein interaction and localization. UNC119A has 2 variants, UNC119Aa and UNC119Ab. UNC119Aa and UNC119Ab have 240 and 220 amino acids, respectively. The N-terminal 204 amino acids are shared by UNC119Aa and UNC119Ab. UNC119B is composed of 251 amino

acids. The N-terminal 59 amino acids of UNC119A diverge from the N-terminal 67 amino acids of UNC119B, whereas the middle portions of UNC119A and UNC119B are well conserved. Therefore, RASSF6 is likely to bind to the N-terminal region of UNC119A.

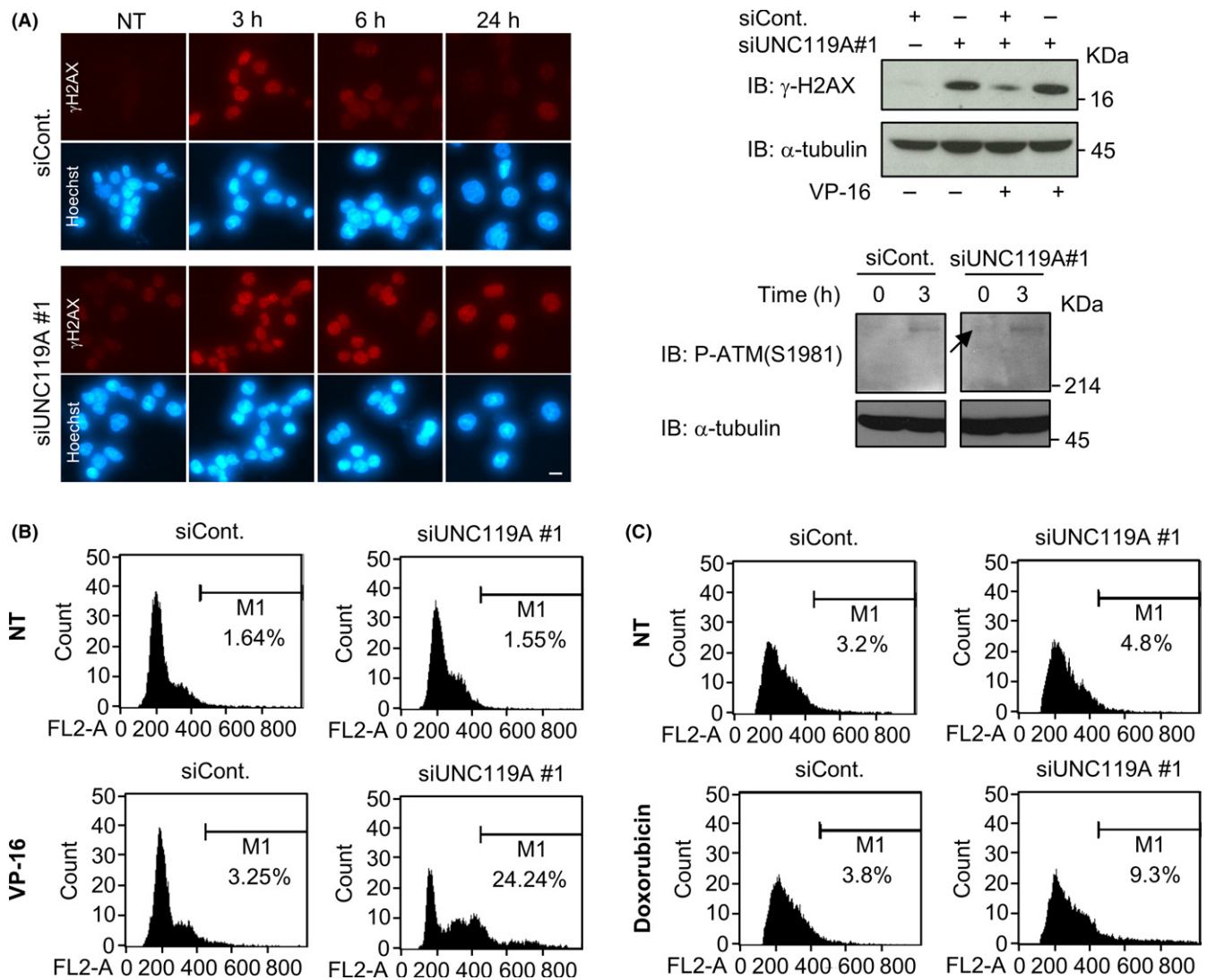


FIGURE 8 UNC119A depletion enhances genomic instability. A-C, HCT116 cells were transfected with control or *UNC119A*-targeted siRNA. 72 h later, cells were exposed to 50 μ M VP-16 for 3 h and returned to the medium without VP-16. In (A), cells were fixed and immunostained with anti- γ -H2AX antibody at the indicated time points. Nuclei were visualized with Hoechst 33342. Cell lysates after 24 h were immunoblotted with anti- γ -H2AX and anti-phospho-ATM antibodies. γ -H2AX and phosphorylated ATM were detected in *UNC119A*-depleted cells without VP-16 treatment (an arrow). In (B), cells were harvested at 96 h. DNA content was analyzed by FACS as described for Figure 3C. In (C), cells were treated with 0.1 μ M doxorubicin for 24 h after siRNA transfection and were cultured for 72 h in the absence of doxorubicin

Overexpression of the full-length *UNC119A* causes apoptosis and cell-cycle arrest in p53-positive HCT116 cells, whereas *UNC119A* depletion attenuates UV-induced apoptosis and cancels UV-induced cell cycle arrest (Figures 3, 4, and 5). These properties are reminiscent of the regulation of apoptosis and cell-cycle progression by *RASSF6*.¹⁷ The underlying mechanism of the tumor-suppressive role of *RASSF6* is not yet fully understood, but one of the important mechanisms is the inhibition of MDM2-mediated degradation of p53. *UNC119A*-mediated apoptosis and cell-cycle arrest also depend on p53. Mechanistically, *UNC119A* enhances the interaction of *RASSF6* and MDM2, reduces p53 ubiquitination, and enhances p53 protein expression (Figures 6 and 7). These findings suggest that *UNC119A* is implicated in the regulation of the *RASSF6*-

MDM2-p53 axis. However, *UNC119A* also induces apoptosis and inhibits BrdU incorporation in HCT116 p53^{-/-} cells, suggesting that *UNC119A* can, to some extent, regulate apoptosis and cell-cycle arrest by a certain mechanism, which is independent of p53. We also observed that exogenously expressed *UNC119A* is detected and interacts with *RASSF6* not only in the cytoplasm but also in the nucleus. As *RASSF6* interacts with MDM2 mainly in the nucleus, it is intriguing to study how the subcellular distribution of *UNC119A* is regulated.

UNC119A was originally reported as a human retina-enriched gene product but is ubiquitously expressed in various tissues. In the retina, *UNC119A* binds transducin and RIBEYE, and plays critical roles in ribbon synapse formation.^{25,26} In hematopoietic cells,

UNC119A interacts with tyrosine kinases—Fyn, Lck, and Lyn—to regulate T-cell activation, eosinophil survival, and the production of cytokines.^{30–32} In lung fibroblasts, UNC119A promotes myofibroblast differentiation through Fyn.³³ In HeLa cells, UNC119A is localized at centrosomes and the midbody, and controls cytokinesis via

Fyn.³² Thus, UNC119A plays versatile roles in many tissues depending on which lipid-modified protein(s) it interacts with. It is an intriguing question as to which lipid-modified protein is involved in the regulation of the RASSF6-MDM2-p53 axis by UNC119A.

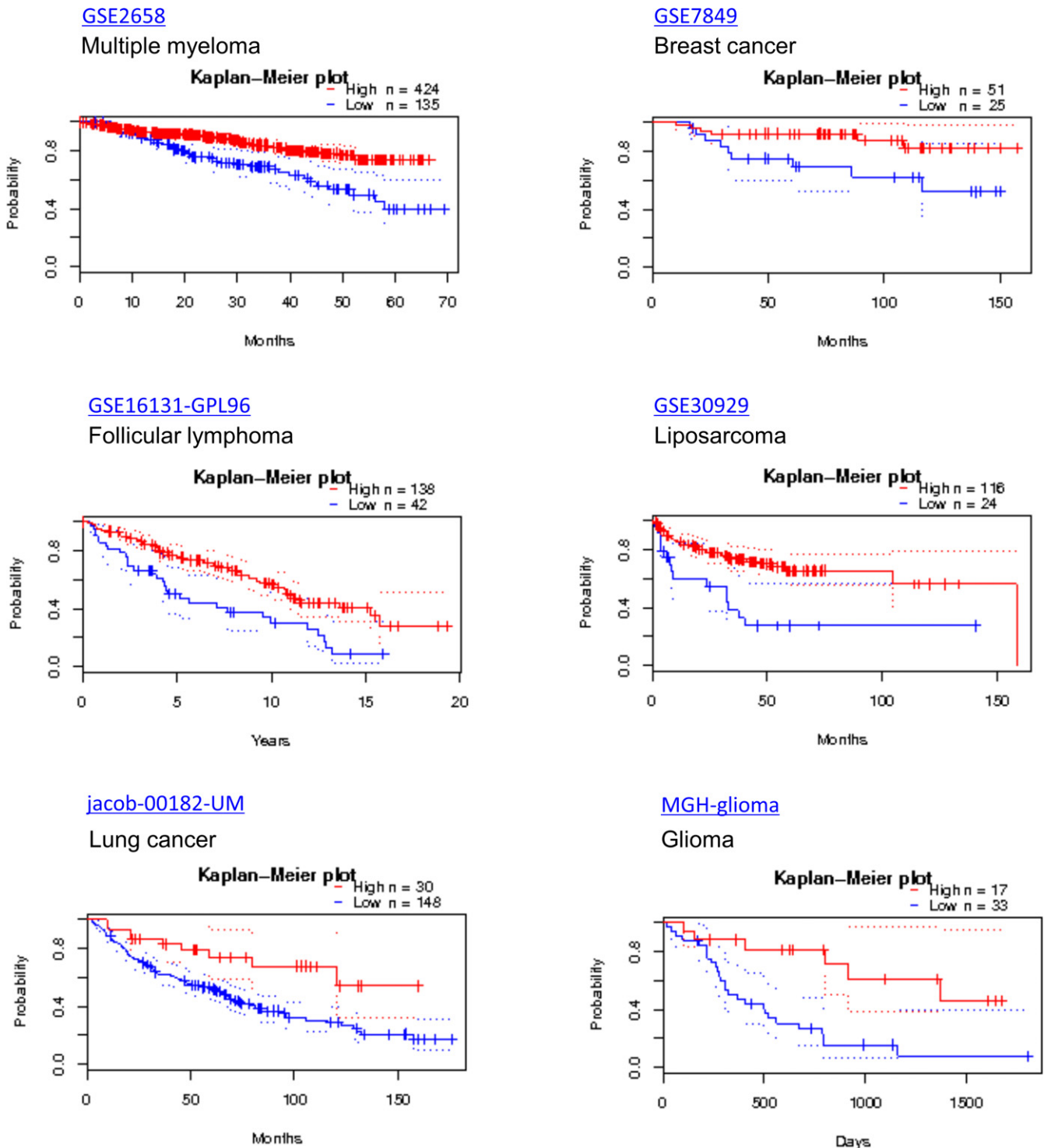


FIGURE 9 Kaplan-Meier plots of cancer patients with high and low expression of UNC119A. High and low UNC119A expression groups were determined according to the criteria of PrognScan database. Kaplan-Meier plots of cancer patients are shown for GSE2658 (multiple myeloma), GSE7849 (breast cancer), GSE16131-GPL96 (follicular lymphoma), GSE30929 (liposarcoma), jacob-00182-UM (lung cancer), and MGH-glioma (glioma). Horizontal axis and vertical axis indicate time and disease-free survival, respectively. Cox *P*-values are shown

RASSF6 suppression by DNA hypermethylation is frequently observed in human cancers and is associated with poor clinical prognosis.³⁴ Stabilization of p53 is an important mechanism by which RASSF6 exerts its tumor-suppressive function. In the present study, we show that UNC119A depletion impairs DNA repair after DNA damage induced by VP-16 and doxorubicin (Figure 8B,C). These findings suggest that UNC119A shows a tumor-suppressive role through p53 in cancer cells. Consistently, low expression of UNC119A is associated with poor prognosis in cancer patients (Figure 9). Among 91 datasets that provided information regarding UNC119A, 6 datasets showed correlation of the low expression of UNC119A with shorter survival. This ratio is apparently not high, but we need to consider the possibility that UNC119A cannot completely suppress tumor without intact RASSF6 and p53. Interestingly, high expression of UNC119A is associated with a poor prognosis in hepatocellular carcinoma.³⁵ In 2 datasets of the PrognScan database (GSE9893, breast cancer; and GSE11595, esophageal cancer), high UNC119A expression is associated with poor prognosis. As UNC119A activates SRC kinases, in cancers with dysregulation of RASSF6 or p53, it is possible that UNC119A rather promotes tumors. To confirm the importance of UNC119A as a tumor suppressor in human cancers, further studies are awaited.

ACKNOWLEDGMENTS

We gratefully acknowledge Feng Zhang and Akira Kikuchi for materials. A.S., S.H., and X.X. are supported by the MEXT scholarship. This work was supported by research grants from Japan Society for the Promotion of Science (JSPS) (26460359, 26293061).

CONFLICTS OF INTEREST

Authors declare no conflicts of interest for this article.

ORCID

Yutaka Hata  <http://orcid.org/0000-0003-1304-5286>

REFERENCES

- Avruch J, Xavier R, Bardeesy N, et al. RASSF family of tumor suppressor polypeptides. *J Biol Chem*. 2009;284:11001-11005.
- Volodko N, Gordon M, Salla M, Ghazaleh HA, Baksh S. RASSF tumor suppressor gene family: biological functions and regulation. *FEBS Lett*. 2014;588:2671-2684.
- Donninger H, Schmidt ML, Mezzanotte J, Barnoud T, Clark GJ. Ras signaling through RASSF proteins. *Semin Cell Dev Biol*. 2016;58:86-95.
- Richter AM, Pfeifer GP, Dammann RH. The RASSF proteins in cancer: from epigenetic silencing to functional characterization. *Biochim Biophys Acta*. 2009;1796:114-128.
- Iwasa H, Hossain S, Hata Y. Tumor suppressor C-RASSF proteins. *Cell Mol Life Sci*. 2018;75:1773-1787.
- Sherwood V, Recino A, Jeffries A, Ward A, Chalmers AD. The N-terminal RASSF family: a new group of Ras-association-domain-containing proteins, with emerging links to cancer formation. *Biochem J*. 2010;425:303-311.
- Underhill-Day N, Hill V, Latif F. N-terminal RASSF family: RASSF7-RASSF10. *Epigenetics*. 2011;6:284-292.
- Dammann R, Li C, Yoon JH, Chin PL, Bates S, Pfeifer GP. Epigenetic inactivation of a RAS association domain family protein from the lung tumour suppressor locus 3p21.3. *Nat Genet*. 2000;25:315-319.
- Liu L, Tommasi S, Lee DH, Dammann R, Pfeifer GP. Control of microtubule stability by the RASSF1A tumor suppressor. *Oncogene*. 2003;22:8125-8136.
- Dalloy A, Agathangelou A, Fenton SL, et al. RASSF1A interacts with microtubule-associated proteins and modulates microtubule dynamics. *Cancer Res*. 2004;64:4112-4116.
- Song MS, Song SJ, Ayad NG, et al. The tumour suppressor RASSF1A regulates mitosis by inhibiting the APC-Cdc20 complex. *Nat Cell Biol*. 2004;6:129-137.
- Vos MD, Martinez A, Elam C, et al. A role for the RASSF1A tumor suppressor in the regulation of tubulin polymerization and genomic stability. *Cancer Res*. 2004;64:4244-4250.
- Song MS, Song SJ, Kim SY, Oh HJ, Lim DS. The tumour suppressor RASSF1A promotes MDM2 self-ubiquitination by disrupting the MDM2-DAXX-HAUSP complex. *EMBO J*. 2008;27:1863-1874.
- Oh HJ, Lee KK, Song SJ, et al. Role of the tumor suppressor RASSF1A in Mst1-mediated apoptosis. *Cancer Res*. 2006;66:2562-2569.
- Guo W, Cui L, Wang C, et al. Decreased expression of RASSF1A and up-regulation of RASSF1C is associated with esophageal squamous cell carcinoma. *Clin Exp Metastasis*. 2014;31:521-533.
- Matallanas D, Romano D, Yee K, et al. RASSF1A elicits apoptosis through an MST2 pathway directing proapoptotic transcription by the p73 tumor suppressor protein. *Mol Cell*. 2007;27:962-975.
- Iwasa H, Kudo T, Maimaiti S, et al. The RASSF6 tumor suppressor protein regulates apoptosis and the cell cycle via MDM2 protein and p53 protein. *J Biol Chem*. 2013;288:30320-30329.
- Ikeda M, Kawata A, Nishikawa M, et al. Hippo pathway-dependent and -independent roles of RASSF6. *Sci Signal*. 2009;2:ra59.
- Maduro M, Pilgrim D. Identification and cloning of unc-119, a gene expressed in the *Caenorhabditis elegans* nervous system. *Genetics*. 1995;141:977-988.
- Higashide T, McLaren MJ, Inana G. Localization of HRG4, a photoreceptor protein homologous to Unc-119, in ribbon synapse. *Invest Ophthalmol Vis Sci*. 1998;39:690-698.
- Kobayashi A, Higashide T, Hamasaki D, et al. HRG4 (UNC119) mutation found in cone-rod dystrophy causes retinal degeneration in a transgenic model. *Invest Ophthalmol Vis Sci*. 2000;41:3268-3277.
- Wright KJ, Baye LM, Olivier-Mason A, et al. An ARL3-UNC119-RP2 GTPase cycle targets myristoylated NPHP3 to the primary cilium. *Genes Dev*. 2011;25:2347-2360.
- Swanson DA, Chang JT, Campochiaro PA, Zack DJ, Valle D. Mammalian orthologs of *C. elegans* unc-119 highly expressed in photoreceptors. *Invest Ophthalmol Vis Sci*. 1998;39:2085-2094.
- Kobayashi A, Kubota S, Mori N, McLaren MJ, Inana G. Photoreceptor synaptic protein HRG4 (UNC119) interacts with ARL2 via a putative conserved domain. *FEBS Lett*. 2003;534:26-32.
- Constantine R, Zhang H, Gerstner CD, Frederick JM, Baehr W. Uncoordinated (UNC)119: coordinating the trafficking of myristoylated proteins. *Vision Res*. 2012;75:26-32.
- Alpadi K, Magupalli VG, Käppel S, et al. RIBEYE recruits Munc119, a mammalian ortholog of the *Caenorhabditis elegans* protein unc119, to synaptic ribbons of photoreceptor synapses. *J Biol Chem*. 2008;283:26461-26467.
- Withanage K, Nakagawa K, Ikeda M, et al. Expression of RASSF6 in kidney and the implication of RASSF6 and the Hippo pathway in the sorbitol-induced apoptosis in renal proximal tubular epithelial cells. *J Biochem*. 2012;152:111-119.

28. Sarkar A, Iwasa H, Hossain S, et al. Domain analysis of Ras-association domain family member 6 upon interaction with MDM2. *FEBS Lett.* 2017;591:260-272.
29. Mizuno H, Kitada K, Nakai K, Sarai A. PrognScan: a new database for meta-analysis of the prognostic value of genes. *BMC Med Genomics.* 2009;2:18.
30. Cen O, Gorska MM, Stafford SJ, Sur S, Alam R. Identification of UNC119 as a novel activator of SRC-type tyrosine kinases. *J Biol Chem.* 2003;278:8837-8845.
31. Palacios EH, Weiss A. Function of the Src-family kinases, Lck and Fyn, in T-cell development and activation. *Oncogene.* 2004;23:7990-8000.
32. Gorska MM, Liang Q, Karim Z, Alam R. Uncoordinated 119 protein controls trafficking of Lck via the Rab11 endosome and is critical for immunological synapse formation. *J Immunol.* 2009;183:1675-1684.
33. Vepachedu R, Gorska MM, Singhania N, Cosgrove GP, Brown KK, Alam R. Unc119 regulates myofibroblast differentiation through the activation of Fyn and the p38 MAPK pathway. *J Immunol.* 2007;179:682-690.
34. Iwasa H, Jiang X, Hata Y. RASSF6; the putative tumor suppressor of the RASSF family. *Cancers (Basel).* 2015;7:2415-2426.
35. Lei B, Chai W, Wang Z, Liu R. Highly expressed UNC119 promotes hepatocellular carcinoma cell proliferation through Wnt/ β -catenin signaling and predicts a poor prognosis. *Am J Cancer Res.* 2015;5:3123-3134.

SUPPORTING INFORMATION

Additional supporting information may be found online in the Supporting Information section at the end of the article.

How to cite this article: Iwasa H, Sarkar A, Shimizu T, et al. UNC119 is a binding partner of tumor suppressor Ras-association domain family 6 and induces apoptosis and cell cycle arrest by MDM2 and p53. *Cancer Sci.* 2018;109:2767–2780. <https://doi.org/10.1111/cas.13706>